Operation of off-grid power supply system using iot monitoring platform for oil and gas pipeline based on RESOC

Xu, Chenxing; Wu, Jian; Feng, Hailin; Ibrom, Andreas; Zeng, Qing; Zhang, Jianfeng; Li, Na; Hu, Qiang

Published in:
CSEE Journal of Power and Energy Systems

Link to article, DOI:
10.17775/cseejpes.2019.01580

Publication date:
2020

Document Version
Publisher's PDF, also known as Version of record

Operation of Off-grid Power Supply System Using IoT Monitoring Platform for Oil and Gas Pipeline Based on RESOC

Chenxing Xu, Jian Wu, Hailin Feng, Andreas Ibrom, Qing Zeng, Jianfeng Zhang, Na Li, and Qiang Hu

***Abstract*—An oil and gas pipeline monitoring platform uses internet of things (IoT) to ensure safe operation in remote and unattended areas, through automatic monitoring and systematic control on equipment such as the cut-off valves and cathodic protection systems. The continuity and stability of power supplies for various equipment of an oil and gas pipeline IoT monitoring platform is crucial. There is no single universal off-grid power supply method that is optimal for an oil and gas pipeline IoT monitoring platform in all different contexts. Therefore, it is necessary to select a suitable one according to the specific geographical location and meteorological conditions. This paper proposes an off-grid power supply system comprised of a reversible solid oxide fuel cell (RESOC), photovoltaic (PV) and battery. Minimum operating costs and the reliability of system operations under constraint conditions are the key determining objectives. A "PV + battery + RESOC" system operational optimization model is established. Based on the model, three types of off-grid power supply schemes are proposed, and three geographical locations with different meteorological conditions are selected as practical application scenarios. The Matlab Cplex solver is used to solve the different power supply modes of the three regions. And finally, the power supply scheme with the best reliability and economy under different geographical environments and meteorological conditions is obtained.**

***Index Terms*—IoT, oil and gas pipeline, off-grid power supply system, operational optimization, reversible solid oxide fuel cell.**

I. Introduction

CHINA'S energy structure is in a stage of deep adjustment. Oil and gas consumption continues to grow. In 2018, the total annual consumption of oil was 4.64 billion tons, an increase of 3.3% over the previous year [1]. The annual consumption of natural gas was 276.6 billion cubic meters, an increase of 16.6% over the previous year [2]. The growth of oil and gas consumption has led to the continued expansion of pipelines. These pipelines include refined oil, crude oil, and natural gas pipelines. The total length of pipelines increased from 93,000 km in 2011 to 133,100 km in 2017 [3]. By 2020, the mileage of three pipelines is expected to reach 32,000 km, 33,000 km, and 104,000 km, respectively. By 2025, the national oil and gas pipeline network is expected to reach 240,000 km [4].

Oil and gas pipelines are mostly distributed in the wild or sea. While oil and natural gases are flammable, explosive, and volatile [5], oil and gas leakages not only cause energy waste, but also explosions, fires, and other accidents. As the size of oil and gas pipelines grows, the safety of pipeline transportation becomes more important. The internet of things (IoT) monitoring platform was created to ensure the safe operation of oil and gas pipelines. The platform utilizes advanced IoT technology and other technologies combined with the original SCADA (supervisory control and data acquisition) system to realize real-time monitoring and regulation management of shut-off valves and cathodic protection devices for oil and gas pipelines. The IoT monitoring platform includes an important load device, which requires a continuous and reliable power supply system [6].

The oil and gas pipeline power supply scheme [7] is primarily divided into three types: grid power supply (with a reliable external grid power supply), grid power supply + battery power supply (unreliable external grid power supply), PV or generator plus battery power supply (no external grid power supply area). Traditional oil and gas pipeline power supply system [8], [9] primarily include grid power supply, photovoltaic (PV) power generation [5], [10], wind and solar hybrid power generation [11]–[15]. Due to climate and other uncontrollable factors, photovoltaic and wind-power generation have each proven to be too volatile and intermittent. Persistent rainy weather creates a substantial risk of power failure. The capacity of the backup battery is limited by space requirements and is also affected by the ambient temperature. A backup battery alone cannot meet the requirements of a continuous and reliable power supply in oil and gas pipelines.

Research on the power supply of oil and gas pipelines has been carried out at home and abroad. Domestic, Sinopec's Zhu Yifei and others analyzed the application of a photovoltaic

Manuscript received July 14, 2019; revised September 30, 2019; accepted November 25, 2019. Date of publication March 30, 2020; date of current version December 24, 2019.

This work was supported by the Zhejiang A&F University Talent Startup Project (2017FR025), the Science and Technology Project in Jinyun (JYKJZDSJ-2018-1), and the Key R&D Program of Sichuan Province (2017GZ0391).

C. X. Xu, J. Wu (corresponding author, email: wujian@zafu.edu.cn), H. L. Feng and J. F. Zhang are with the College of Information Engineering, Zhejiang A&F University, Hangzhou 311300, China.

A. Ibrom is with the Department of Environmental Engineering, Technical University of Denmark, 2800 Kgs. Lyngby, Denmark.

Q. Zeng is with the Tsinghua Sichuan Energy Internet Research Institute, Chengdu 610213, China.

N. Li is with the CRRC Wind Power (Shandong) Co., Ltd, Representative Office in Denmark, Roskilde 4000, Denmark.

Q. Hu is with the Zhejiang Zhentai Energy Technology Co. Ltd., Lishui 323000, China.

DOI: 10.17775/CSEEJPES.2019.01580

power generation system in the Shengli Oilfield [5]; Southern Petroleum's Xue Guangmin and others used Fushan Oilfield as an example to introduce the application of a photovoltaic power generation system in remote well sites [16]; Oil Group's Yu Yurui studied the wind-solar hybrid power generation system used in long-distance pipelines and believe that the system can improve the reliability of the power supply and reduce the operating costs of the system [17]. Abroad, Greenblartt Research believes that renewable energy generators can replace fuel generators. Natural gas pipeline power supply can improve economic and environmental benefits [18]. Johnson *et al.* used photovoltaic power generation combined with batteries to power oil and gas pipeline monitoring platforms [19]. Pharris and Kolpa studied photovoltaic power generation systems that supply power to pipeline cathodic protection stations [20].

Proton exchange membrane fuel cells (PEMFC) have been currently used more frequently in such hybrid off-grid power systems due to the advantages of high-power generation efficiency, high-energy density, strong endurance, no pollution, no noise, and convenient installation and use. Compared with PEMFC, reversible solid oxide fuel cells (RESOC) are another type of fuel cell, and could be more advantageous when used for off-grid power supply in remote areas. Several comparisons are made below:

1) PEMFC is a low-temperature fuel cell (operating temperature is between 60–80°C) [21], which is prone to problems in certain environments like alpine-cold regions. RESOC is a high-temperature fuel cell (operating temperature is around 600–1000°C) [22]. In alpine-cold regions where many oil and gas pipelines were distributed, RESOC can sustain ambient temperatures and ensure more stable operations of the equipment.

2) RESOC can be used in both solid oxide fuel cell (SOFC) mode and solid oxide electrolyzer cell (SOEC) mode, thus it has a potential to reduce system complexity and cost.

3) RESOC has a certain carbon tolerance, whereas PEMFC requires extremely high purification of the fuel. Therefore, RESOC has better adaptability to fuel and a higher reliability.

At present, there are very few studies addressing the application of RESOC in oil and gas pipeline power supply systems. Therefore, this paper proposes an off-grid power supply system based on RESOC for an oil and gas pipeline IoT monitoring platform. The system includes PV, batteries, RESOC, and hydrogen storage tanks. For the proposed system, the power model of each component and the operating characteristic model of RESOC are well established. The operational characteristics model examines the relationship between temperature, power generation, and heat generation. Finally, with the objective function of the system being minimum operating cost and the constraint being reliability of system operation, the optimal operational model of the system is established.

Since an oil and gas pipeline IoT monitoring platform needs to choose a suitable power supply scheme according to their geographical location and meteorological conditions, this paper is based on the China solar irradiance distribution map published by NREL and the distribution map of China's oil and gas pipelines, and selects three regions with different irradiance levels and ambient temperatures. Three types of power supply configuration methods are designed: PV + Battery, PV + Battery + RESOC, and PV + RESOC. The MatlabCplex solver is used to solve the optimization model and the power supply scheme with the best reliability and economy under different geographical environments and meteorological conditions is obtained.

The rest of this paper is organized as follows: Section II describes the mathematical model of photovoltaic, battery, RESOC, hydrogen storage tanks, etc. Section III proposes an optimization model for the off-grid power supply system. Section IV designs three configuration methods of power sources for the oil and gas pipeline IoT monitoring platform and selects three typical regional data for case analysis, and the conclusion is drawn in Section V.

II. Off-grid Power Supply System Model

A. System Structure

A RESOC based off-grid power supply system for an oil and gas pipeline IoT monitoring platform includes components such as a PV, a battery, a SOFC and SOEC, and a hydrogen storage tank; and its structure is shown in Fig. 1. According to different geographical environments and climate conditions, three schemes are designed. Scheme 1 is [PV + Battery]; scheme 2 is [PV + Battery + RESOC]; and scheme 3 is [PV + RESOC]. MatlabCplex is used to optimize the operations of the three configuration schemes. Finally, the power supply scheme with the best reliability and economy under different geographical environments and meteorological conditions is obtained.

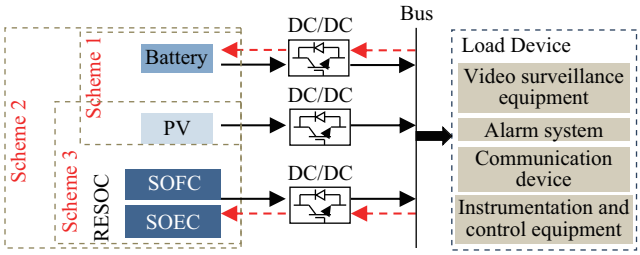

Fig. 1. Off-grid power generation system structure.

B. Photovoltaic Power Generation Model

Photovoltaic power generation is a power supply system that uses photovoltaic semiconductor materials to convert solar energy into direct current electrical energy. Its core device is a solar photovoltaic panel. The output characteristics of photovoltaic panels are nonlinear, depending on solar radiation intensity, ambient temperature, and special operating point [23], [24].

The ideal operating point of a photovoltaic module under different environmental conditions is when the output power is at the maximum power point, which can be achieved by appropriately controlling the power electronic converter at the output. For this study, the output power of a photovoltaic module can be determined by the following equation [23]:

$$P_{\mathrm{PV}} = \eta_{\mathrm{PV}} \cdot H \cdot A \tag{1}$$

where η_{PV} is the output efficiency of the photovoltaic system. H (W/m^2) is the solar radiation, and A (m^2) is the total area of the photovoltaic components. This article uses the actual amount of solar radiation per hour to calculate the rate of output power per hour.

C. Reversible Solid Oxide Fuel Cell

1) Solid Oxide Fuel Cell Model

SOFC can supply equipment with power for several days, weeks or even months by converting chemical energy into electrical energy. It is a high-operating-temperature (600–1000°C), high-energy-density, high-energy-converting (about 60%) [25], low-fuel (hydrocarbon fuel), environmentally-friendly, and long-term backup power supply. Its working principle is shown in Fig. 2.

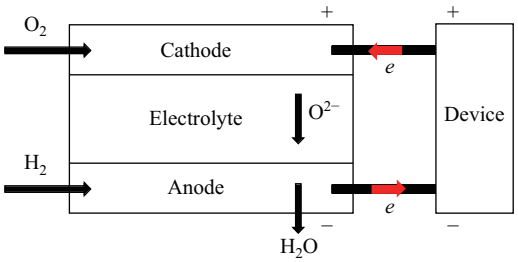

Fig. 2. Schematic diagram of the working principle of SOFC mode.

The total reaction equation for SOFC can be expressed as:
Oxygen electrode (cathode): $1/2\mathrm{O}_2 + 2\mathrm{e}^- \rightarrow \mathrm{O}^{2-}$
Hydrogen electrode (anode): $\mathrm{H}_2 + \mathrm{O}^{2-} \rightarrow \mathrm{H}_2\mathrm{O} + 2\mathrm{e}^-$
Total response: $\mathrm{H}_2 + 1/2\mathrm{O}_2 \rightarrow \mathrm{H}_2\mathrm{O}$
From the first law of thermodynamics and the second law:

$$\Delta G = \Delta H - T\Delta S \tag{2}$$

where ΔG is the Gibbs free energy change of the reaction ($\Delta G < 0$ in SOFC, $\Delta G > 0$ in SOEC). ΔH is the reaction enthalpy. T is the Kelvin temperature of the reaction, and ΔS is the entropy change for the reaction.

In the case where all electrons passing through the battery participate in the reaction, ΔH can be expressed as the thermal neutral voltage E_{tn} during the reaction [26]:

$$E_{\mathrm{th}} = \frac{\Delta H}{nF} \tag{3}$$

where n is the number of moles of electrons participating in the reaction. F is the Faraday constant.

In the actual operation of the SOFC, since the electrochemical reaction inside the battery is irreversible, there will inevitably be some loss, resulting in loss of polarization (also called voltage loss). Polarization loss is divided into electrode reaction polarization loss E_{act}, and battery ohmic resistance polarization loss E_{ohm}, both of which are related to temperature. E_{act} increases linearly with current density i, and E_{ohm} increases logarithmically. Therefore, the voltage of the SOFC can be described as a function of temperature and current density as:

$$E_{\mathrm{SOFC}} = f(i,T) = E_{\mathrm{rev}}(T) + E_{\mathrm{act}}(i,T) + E_{\mathrm{ohm}}(i,T) \tag{4}$$

where E_{rev} is the reversible electromotive force of the battery reaction.

The output power of the SOFC can be solved by the following equation:

$$W_{\mathrm{SOFC}} = n \cdot F \cdot E_{\mathrm{SOFC}} \tag{5}$$

$$P_{\mathrm{SOFC}} = \eta_{\mathrm{SOFC}} \cdot P_{\mathrm{H_2\_out}} \tag{6}$$

where W_{SOFC} is the work output for the SOFC battery. η_{SOFC} is the SOFC discharge efficiency, and $P_{\mathrm{H_2\_out}}$ is the hydrogen power input to the fuel cell from the hydrogen tank.

2) Solid Oxide Electrolytic Cell Model

The SOEC is an energy conversion device that converts electrical energy and thermal energy into chemical energy, and has the advantages of high energy conversion efficiency (about 90%) [27], high current density, zero pollution, and no noise. SOEC is composed of three parts: oxygen electrode (anode), electrolyte, and hydrogen electrode (cathode). The working principle diagram is shown in Fig. 3.

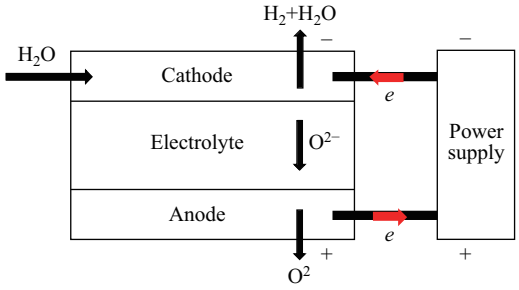

Fig. 3. Schematic diagram of the working principle of SOEC mode.

The total reaction equation for SOEC can be expressed as:
Hydrogen electrode (cathode): $\mathrm{H}_2\mathrm{O} + 2\mathrm{e}^- \rightarrow \mathrm{H}_2 + \mathrm{O}^{2-}$
Oxygen electrode (anode): $\mathrm{O}^{2-} \rightarrow 1/2\mathrm{O}_2 + 2\mathrm{e}^-$
Total response: $\mathrm{H}_2\mathrm{O} \rightarrow \mathrm{H}_2 + 1/2\mathrm{O}_2$
The terminal voltage of SOEC can be expressed as [27]

$$E_{\mathrm{SOEC}} = f(i,T) = E_{\mathrm{rev}}(T) + E_{\mathrm{act}}(i,T) + E_{\mathrm{ohm}}(i,T) \tag{7}$$

The output power of SOEC can be solved by the following equations:

$$W_{\mathrm{SOEC}} = n \cdot F \cdot E_{\mathrm{SOEC}} \tag{8}$$

$$\eta_{\mathrm{SOEC}} = \frac{\Delta H}{W_{\mathrm{SOEC}}} = \frac{E_{\mathrm{th}}}{E_{\mathrm{SOEC}}} \tag{9}$$

$$P_{\mathrm{H_2\_in}} = P_{\mathrm{SOEC}} \cdot \eta_{\mathrm{SOEC}} \tag{10}$$

where W_{SOEC} is the work done for the SOEC output. $P_{\mathrm{H_2\_in}}$ is the power of the hydrogen output from the electrolysis cell. P_{SOEC} is the output power of the electrolytic cell, and η_{SOEC} is the conversion efficiency of the SOEC.

D. Hydrogen Storage Tank Model

The low density and low boiling point of hydrogen make it difficult to store. Hydrogen is typically stored in a metal oxide under high pressure. The capacity of the hydrogen storage tank (W · h) can be expressed as [28]:

$$E_{\mathrm{tank}}(t) = E_{\mathrm{tank}}(t-1) + P_{\mathrm{H_2\_in}} \cdot \Delta t - \frac{P_{\mathrm{H_2\_out}}}{\eta_{\mathrm{tank}}} \cdot \Delta t \tag{11}$$

where $E_{\mathrm{tank}}(\mathrm{t})$ and $E_{\mathrm{tank}}(\mathrm{t}-1)$ is the storage capacity of the hydrogen storage tank at times t and $t-1$. Δt is the time interval, and η_{tank} is the efficiency of the tank to store hydrogen.

E. Battery Model

The function of the battery is to store the extra energy of the solar module. When the solar power is insufficient, the battery is discharged for use by the device. The storage capacity of the battery usually needs to be set according to the load demand during the solar non-available period. The battery life require-ment is generally 3–5 days. The size of the battery pack also needs to consider factors such as maximum discharge depth, rated battery capacity, and battery life. The total capacity ($\mathrm{W}\cdot\mathrm{h}$) of the battery pack can be expressed as:

$$E_{\mathrm{Bat}} = P_{\mathrm{Load}} \cdot T_{\mathrm{B}} \cdot f_{\mathrm{V}} \cdot f_{\mathrm{C}} \cdot f_{\mathrm{L}} / \sigma_{\mathrm{D}} / f_{\mathrm{M}} / \eta_{\mathrm{L}} \tag{12}$$

where P_{Load} is the load power. T_{B} is the backup time. f_{V} is the temperature coefficient. f_{C} is the capacity compensation coefficient. f_{L} is the life conversion factor. σ_{D} is the maximum depth of discharge of the battery. f_{M} is the plate activation coefficient; and η_{L} is the conversion efficiency of the converter

The charge and discharge capacity of the battery per unit time can be expressed as:

$$E_{\mathrm{Bat\_in}} = P_{\mathrm{Bat\_in}} \cdot \eta_{\mathrm{Bi}} \cdot \Delta t \tag{13}$$

$$E_{\mathrm{Bat\_out}} = P_{\mathrm{Bat\_out}} / \eta_{\mathrm{Bo}} \cdot \Delta t \tag{14}$$

where $E_{\mathrm{Bat\_in}}$ is the battery charge ($\mathrm{W}\cdot\mathrm{h}$). $P_{\mathrm{Bat\_in}}$ is the battery charge power (W). η_{Bi} is the battery charging efficiency, $E_{\mathrm{Bat\_out}}$ is the battery discharge capacity ($\mathrm{W}\cdot\mathrm{h}$). $P_{\mathrm{Bat\_out}}$ is the battery discharge power (W), and η_{Bo} is the discharge efficiency of the battery.

The minimum remaining capacity of the battery can be exprssed as:

$$E_{\mathrm{D}} = E_{\mathrm{Bat}} \cdot (1 - \sigma_{\mathrm{D}}) \tag{15}$$

where σ_{D} is the maximum depth of discharge of the battery.

Battery operation can be adversely affected by extreme ambient temperatures. The optimal operating temperature is 25°C. If the battery operates at a temperature lower than 5°C or higher than 40°C for prolonged periods [29], battery life will be compromised. Compared with an ideal operating temperature of 25°C, as the ambient temperature decreases, battery capacity changes, though not linearly. The rate of change in capacity is directly related to the quality of the battery. Its relative capacity is affected by temperature [30] as shown in Fig. 4. The relative discharge capacity of the battery can be expressed as:

$$R_{\mathrm{T}} = R_{25} - \sigma_{\mathrm{T}}(25 - T_{\mathrm{R}}) \tag{16}$$

where R_{25} is battery relative discharge capacity at standard temperature 25°C. σ_{T} is the temperature coefficient of capacity, and T_{R} is the ambient temperature.

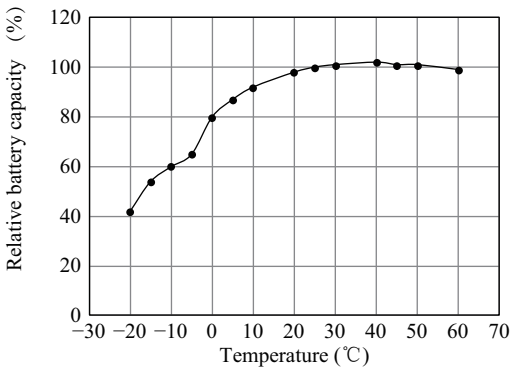

Fig. 4. Relative capacity of battery with temperature curve.

III. Off-Grid Power Supply System OperationAL Optimization Model

A. Optimizing the Objective Function

The operational optimization goal of the system is to find the minimum operating cost, while also meeting performance indicators of the off-grid power supply system, which is:

$$\min COST(x) = \sum_{i=1}^{7} \lambda_i \left(\sum_{t=1}^{T_1} x_i \right) \tag{17}$$

where T_1 is the operating cycle of the system (h).

The decision vector $\boldsymbol{x}$ is defined as follows for the present problem:

$$\begin{aligned} \boldsymbol{x} = [&P_{\mathrm{PV,t}}, P_{\mathrm{Bat\_in,t}}, P_{\mathrm{Bat\_out,t}}, P_{\mathrm{SOFC,t}}, \\ &P_{\mathrm{SOEC,t}}, P_{\mathrm{loss,t}}, P_{\mathrm{lack,t}}] \end{aligned} \tag{18}$$

where $P_{\mathrm{PV,t}}$ is the output power per unit time of photovoltaic system. $P_{\mathrm{Bat\_in,t}}$ is the battery input power at time *t*. $P_{\mathrm{Bat\_out,t}}$ is the battery unit time output power. $P_{\mathrm{SOFC,t}}$ is the SOFC unit time output power. $P_{\mathrm{SOEC,t}}$ is the SOEC unit time output power. $P_{\mathrm{loss,t}}$ is the systemabandoned light power per unit time. $P_{\mathrm{lack,t}}$ is the lack of electric power rate per unit time of the system.

$\boldsymbol{\lambda}$ is a collection of system component unit operating costs, which can be expressed as:

$$\boldsymbol{\lambda} = [\lambda_{\mathrm{pv}}, \lambda_{\mathrm{Bat\_in}}, \lambda_{\mathrm{Bat\_out}}, \lambda_{\mathrm{SOFC}}, \lambda_{\mathrm{SOEC}}, \lambda_{\mathrm{loss}}, \lambda_{\mathrm{lack}}] \tag{19}$$

where λ_{pv} is the hourly unit operating cost of the photovoltaic system. $\lambda_{\mathrm{Bat\_in}}$ is the battery unit charging cost per hour. $\lambda_{\mathrm{Bat\_out}}$ is the battery unit discharge cost per hour. λ_{SOFC} is the unit power generation cost per hour of SOFC. λ_{SOEC} is the unit hydrogen production cost of the SOEC. λ_{loss} isthe penalty cost per unit of abandoned light power. λ_{lack} is the unit of power shortage penalty cost.

B. Optimization Constraints

The following constraints must be considered when running an optimized design for an off-grid power system.

1) System Power Balance Constraints

$$\begin{aligned}\Delta P_{\mathrm{t}} &= P_{\mathrm{Load,t}} + P_{\mathrm{gen,t}} - P_{\mathrm{res,t}} + P_{\mathrm{Lack,t}} - P_{\mathrm{Loss,t}} \\ P_{\mathrm{res,t}} &= P_{\mathrm{SOFC,t}} + P_{\mathrm{Bat\_out,t}} \\ P_{\mathrm{gen,t}} &= P_{\mathrm{SOEC,t}} + P_{\mathrm{Bat\_in,t}} \\ \Delta P_{\mathrm{t}} &= 0 \end{aligned} \tag{20}$$

2) Battery Charge and Discharge Power and Charge and Discharge Capacity Constraints

$$0 \le P_{\mathrm{Bat\_in,t}} \le P_{\mathrm{Bat\_in\_max}} \tag{21}$$

$$0 \le P_{\mathrm{Bat\_out,t}} \le P_{\mathrm{Bat\_out\_max}} \tag{22}$$

$$0 \le E_{\mathrm{Bat\_in,t}} \le E_{\mathrm{Bat}} \tag{23}$$

$$E_{\mathrm{D}} \le E_{\mathrm{Bat\_out,t}} \le E_{\mathrm{Bat}} \tag{24}$$

3) SOFC Power Constraints

$$0 \le P_{\mathrm{SOFC,t}} \le P_{\mathrm{SOFC\_max}} \tag{25}$$

4) SOEC Power Constraints

$$0 \le P_{\mathrm{SOEC,t}} \le P_{\mathrm{SOEC\_max}} \tag{26}$$

5) Hydrogen Storage Tank Energy Constraints

$$E_{\mathrm{tank\_max}} \cdot \sigma_{\mathrm{tank}} \le E_{\mathrm{tank,t}} \le E_{\mathrm{tank\_max}} \tag{27}$$

where $P_{\mathrm{Load,t}}$ is the load power (W). $P_{\mathrm{res,t}}$ is the total power generation (W) of the system. $P_{\mathrm{gen,t}}$ is the total storage power (W) of the system. $P_{\mathrm{Bat\_in\_max}}$ is the rated charging power of the battery (W). $P_{\mathrm{Bat\_out\_max}}$ is the rated discharge power (W) of the battery. $P_{\mathrm{SOFC\_max}}$ is the maximum rated power (W) of the SOFC. $P_{\mathrm{SOEC\_max}}$ is the maximum rated power (W) of the SOEC. σ_{tank} is the minimum residual energy coefficient of the hydrogen storage tank. $E_{\mathrm{tank\_max}}$ is the maximum storage capacity (W · h) of the hydrogen storage tank.

IV. Case Analysis

A. Basic Data

The proposed optimization model is used to optimize the operation of the power supply of the off-grid power supply system. The alternative power supply types include photovoltaic modules, storage batteries, SOFC, SOEC, and hydrogen storage tanks. The parameters are shown in Table I, where the Parameter data is from literature [23], [26], [27], [31], [32].

The operating costs of various components of the system are shown in Table II. The operating cycle of the project design is 120 h, and the operating costs in the example are calculated in RMB (Chinese yuan).

There is no one-size-fits-all mode for all oil and gas pipeline IoT monitoring platformpower supply schemes. Based on the geographical location and meteorological conditions of the oil and gas pipeline IoT monitoring platform, a suitable power supply scheme must be chosen [33]. The operational optimization of off-grid power supply systems requires solar irradiance and power load data for each geographic location of the oil and gas pipeline IoT monitoring platform. Three distinct regions (varied by irradiance and climate) were considered in this paper: Sichuan (consecutive rainy days, weak irradiance, non-cold), Ningxia (low levels of rain, strong irradiance, non-cold) and Tibet (low levels of rain, strong irradiance, very cold). The solar irradiance data and temperature variation curves of the three regions are shown in Fig. 5 and Fig. 6. The oil and gas pipeline IoT monitoring platform includes a video monitoring system, an alarm system, communication equipm-

TABLE I
Parameters of the System

Parameter	Symbol	Value
PV efficiency	η_{PV}	17%
Battery backup cycle	T_{B}	72 h
Batterytemperature coefficient	f_{V}	1.1
Battery capacity compensation coefficient	f_{C}	1.1
Battery life conversion factor	f_{L}	1.1
Battery dischargedepth	σ_{D}	80%
Battery plate activation coefficient	f_{M}	1.1
Converter conversion efficiency	η_{L}	91%
Battery charging efficiency	η_{Bi}	90%
Battery discharge efficiency	η_{Bo}	90%
Temperature coefficient of capacity	σ_{T}	0.98%
SOFC efficiency	η_{SOFC}	60%
SOEC efficiency	η_{SOEC}	90%
Tank remaining capacity	σ_{tank}	5%
Tank storage efficiency	η_{tank}	95%

TABLE II
Off-Grid Power System Operating Costs

Component type	C_{ope} (RMB/(W·h))
PV	0
Battery Charging	0.0001
Battery discharge	0.00012
SOFC	0.0003
SOEC	0.0002
PV Curtailment	0.001
Load Shedding	0.01

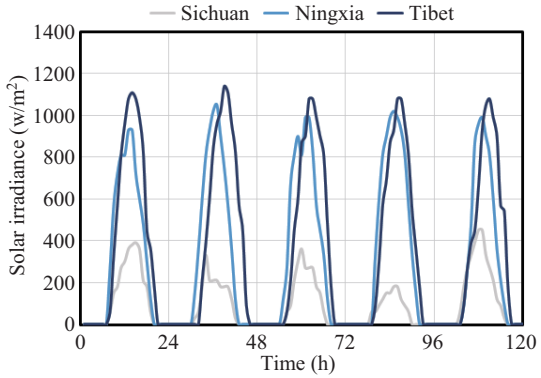

Fig. 5. Variation curve of irradiance in Sichuan, Ningxia and Tibet for 120 h (Data from National Meteorological Information Center).

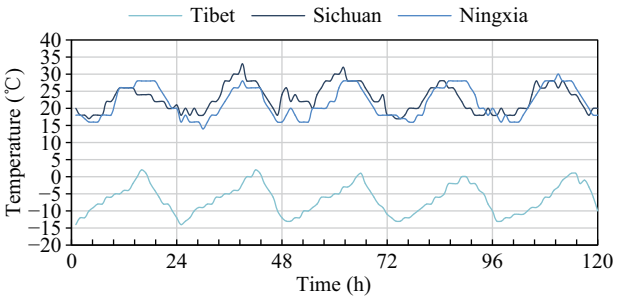

Fig. 6. Temperature curve of Sichuan, Ningxia and Tibet for 120 h. (Data from National Meteorological Information Center).

TABLE III
LOAD INTRODUCTION

Load name	Load power/W	Load level	Power supply time/(h/d)
Video surveillance equipment	125	Important load	24
Intrusion alert device	55	Important load	24
Pipe abnormal alarm device	55	Important load	24
Instrumentation and control equipment	200	Important load	24
communication device	165	Important load	24

ent, and instrumentation and control equipment. Related load introduction is shown in Table III [7], [34], [35]. It is stated in Article 10.1.3 of the Code for Design of a Gas Transmission Pipeline (GB50251-2015) that pipeline power load should be no lower than a Level 2 priority power user. The primary electric load level should be Level 1 priority. Since the primary load of the oil and gas IoT monitoring platformpipeline requires 24 h of uninterrupted power supply and a stable load power demand, the load power is set to 600 W.

For each typical area, three configurations are designed:

1) PV and battery;
2) PV, battery, and RESOC;
3) PV and RESOC.

B. Analysis of Results

1) Analysis of Results in Rainy Weather Areas

This experiment chose Sichuan as a typical representative of rainy weather. There were many continuous rainy days in the area, so solar irradiance was weak. Solar irradiance in a power-deficient area in Sichuan was selected for experimental data. Four different power supply schemes were selected for the area, and the optimized operation of each scheme was studied. The results are shown in Fig. 7.

For Scheme1, PV (20 m^2) + Battery (72 kW · h), when the photovoltaic power generation is zero, the system is powered by the battery. When the photovoltaic power generation is greater than the load, the excess power charges the battery, which stores the energy. According to meteorological data, many areas had as much as 42 consecutive rainy days. Continuous rainy days will result in low photovoltaic power generation and a large amount of battery energy consumption. Battery capacity is limited by physical space conditions. When the battery reaches its maximum discharge depth, the system will experience a power shortage, as shown in Fig. 7 (a). If the oil and gas pipeline IoT monitoring platform powers off, it will result in huge losses. To ensure the reliability of the oil and gas pipeline IoT monitoring platform power supply, photovoltaic panels can be added as in Scheme 2: PV (60 m^2) + Battery (72 kW · h). However, such measures can lead to serious abandoned light power, resulting in large amounts of wasted light resource, as shown in Fig. 7 (b). Another measure would be to increase the storage capacity of the battery, but actual conditions present certain restrictions on battery space, which makes this not feasible. To solve the problem of a power shortage caused by continuous rain, this paper also analyzed Scheme 3: PV (20 m^2) + Battery (72 kW · h) + RESOC (160 kW · h). When there is no solar irradiance, using the battery combined with SOFC to supply power to the system can effectively prevent power shortages. When the photovoltaic output is greater than the load, the battery is charged to store excess energy, and excess photovoltaic power generation can generate hydrogen storage through SOEC, as shown in Fig. 7 (c). This scheme effectively meets the reliability requirements of the system's power supply. Scheme 4 does not include a

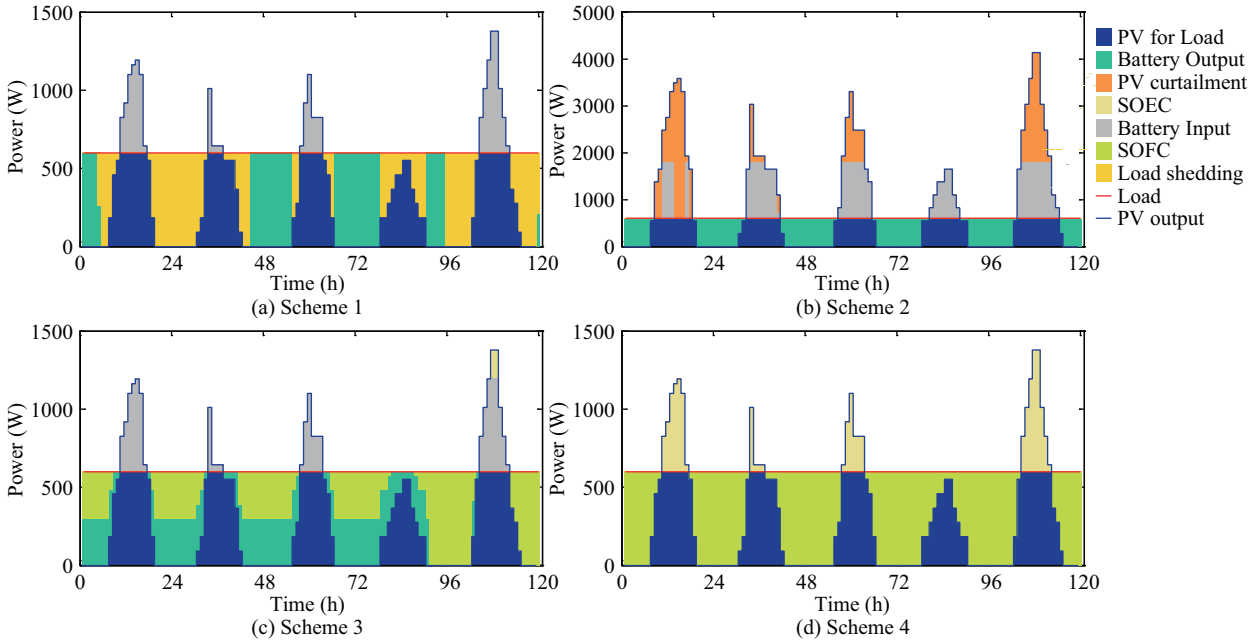

Fig. 7. Optimization results of four schemes in a region of Sichuan.

battery: PV (20 m^2) + RESOC (160 kW · h). When there is no photovoltaic power generation, the SOFC supplies power to the oil and gas pipeline IoT monitoring platform. When the PV is larger than the load, the excess photovoltaic energy is converted into hydrogen by SOEC for storage, as shown in Fig. 7 (d). This scheme can meet the reliability of the oil and gas pipeline IoT monitoring platform power supply, but RESOC's "electric-hydrogen-electric" integrated energy conversion efficiency is low (about 50%), compared with the battery. Also, the RESOC energy storage operational cost is relatively expensive, making it less economic than Scheme 3.

According to the analysis of Table IV, although both satisfy the reliability of the power supply, Scheme 3 is more economical than Scheme 4. Therefore, Scheme 3 (PV + Battery + RESOC) is the preferred solution for many consecutive rainy days.

2) Analysis of Results in Non-cold and Rain-free Areas

Ningxia, as a typical representative of non-cold areas with less rainy weather, had relatively few continuous rainy days and stronger solar irradiance. Solar irradiance in a power-deficient area in Ningxia was selected for experimental data. Three power supply schemes were selected for the region, and the optimized operation of each scheme was studied. The results are shown in Fig. 8.

For Scheme 1, PV (12 m^2) + Battery (72 kW · h), when there is no solar irradiance at night, the battery provides all the required power for the load. When the photovoltaic output is greater than the load during the day, the excess photovoltaic energy is stored by the battery for storage as shown in Fig. 8 (a). Due to the abundant sunshine in the area, there will be some abandoned light power in Scheme 1. In Scheme 2, PV (12 m^2) + Battery (72 kW · h) + RESOC (160 kW · h), when there is no photovoltaic power generation at night, the battery and the SOFC jointly supply power to the oil and gas pipeline IoT monitoring platform. When the photovoltaic output is larger than the load, the excess photovoltaic power generation will be partially stored in the battery, and the remaining SOEC is converted into hydrogen for storage, so there is no unnecessary abandoned light power, as shown in Fig. 8 (b). With Scheme 3, PV (12 m^2) + RESOC (160 kW · h), when the photovoltaic power generation does not meet the load demand, the SOFC supplies power to the oil and gas pipeline IoT monitoring platform; when the amount of photovoltaic power generation is greater than the load, the excess photovoltaic energy is converted to hydrogen by SOEC for storage, as shown in Fig. 8 (c). It can be seen from Fig. 7 that in non-cold areas with strong illumination, Schemes 1, 2, and 3 can all meet the requirements of power supply reliability of the oil and gas pipeline IoT monitoring platform.

The operating costs of power generation for fuel cells (and their storage) are high. Given that all three schemes meet the reliability requirements, it can be shown by combining the

TABLE IV
FOUR CONFIGURATION SCHEMES AND OPERATION OPTIMIZATION RESULTS IN A CERTAIN AREA OF SICHUAN

Schemes	A (m^2)	E_{Bat} (W · h)	Battery power		P_{SOFC} (W)	P_{SOEC} (W)	E_{tank} (W · h)	Operating costs (RMB)
			$P_{\mathrm{Bat\_in}}$ (W)	$P_{\mathrm{Bat\_out}}$ (W)				
Scheme 1	20	72000	1200	600	0	0	0	256.2099
Scheme 2	60	72000	1200	600	0	0	0	40.199
Scheme 3	20	72000	600	300	600	1200	160000	10.8669
Scheme 4	20	0	0	0	600	1200	160000	15.1496

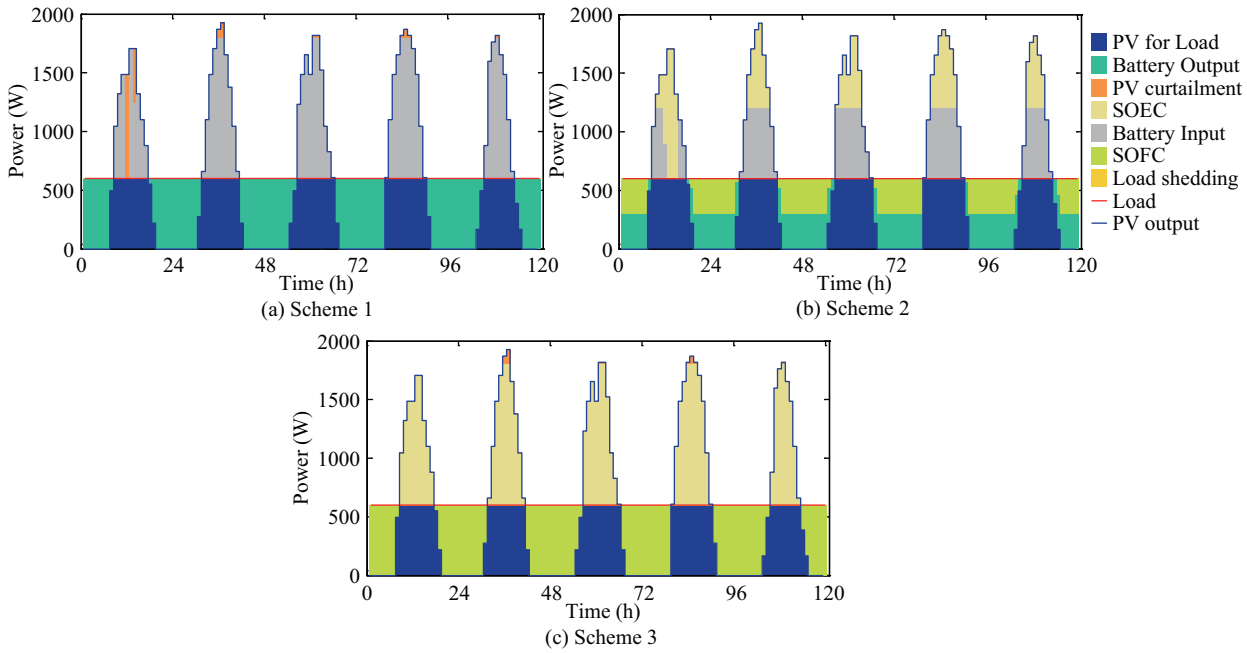

Fig. 8. Optimization results of three schemes in a region of Ningxia.

TABLE V
THREE CONFIGURATION SCHEMES AND OPERATIONAL OPTIMIZATION RESULTS IN A CERTAIN AREA OF NINGXIA

Schemes	A (m^2)	E_{Bat} (W · h)	Battery power		P_{SOFC} (W)	P_{SOEC} (W)	E_{tank} (W · h)	Operating costs (RMB)
			$P_{\mathrm{Bat\_in}}$ (W)	$P_{\mathrm{Bat\_out}}$ (W)				
scheme 1	12	72000	1200	600	0	0	0	9.8622
scheme 2	12	72000	600	300	600	1200	160000	13.138
scheme 3	12	0	0	0	600	1200	160000	19.2763

TABLE VI
THREE CONFIGURATION SCHEMES AND OPERATION OPTIMIZATION RESULTS IN A CERTAIN AREA OF TIBET

Schemes	A (m^2)	E_{Bat} (W · h)	Battery power		P_{SOFC}/(W)	P_{SOEC} (W)	E_{tank} (W · h)	Operating costs (RMB)
			$P_{\mathrm{Bat\_in}}$ (W)	$P_{\mathrm{Bat\_out}}$ (W)				
Scheme 1	10	72000	1200	600	0	0	0	56.1499
Scheme 2	10	72000	600	300	600	1200	160000	11.921
Scheme 3	10	0	0	0	600	1200	160000	17.6974

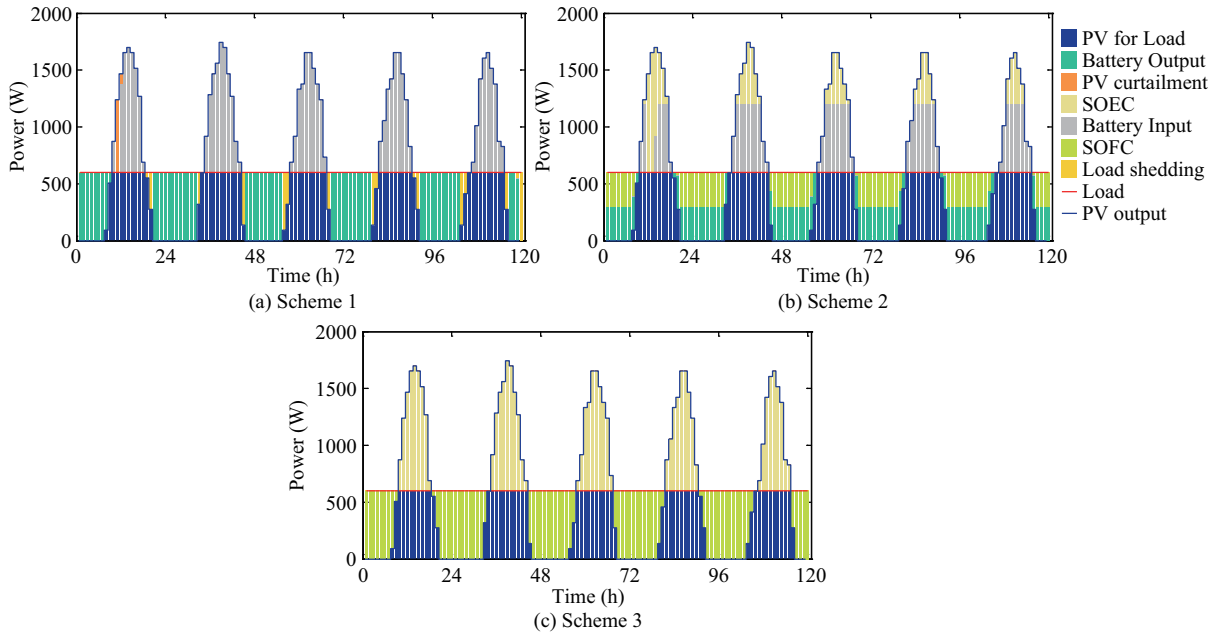

Fig. 9. Operation optimization results of three types of configuration schemes in a certain area of Tibet.

analysis of Table V that the economy of Scheme 1 is superior. Therefore, Scheme 1 (PV + Battery) is a preferred option for non-alpine-coldregionsand areas with less rain.

3) Analysis of Results in Alpine-cold Regions

As a typical representative of alpine-cold regions, Tibet has less rainy days, lower ambient temperatures, and stronger solar irradiance. Solar irradiance in a power-deficient area of Tibet was selected for experimental study. Three types of power supply schemes were selected, and the optimized operation of each scheme was studied. The results are shown in Fig. 9.

For Scheme 1, PV (10 m^2) + Battery (72 kW · h), due to the low ambient temperatures in the area, the effective capacity of the battery will be affected. With Scheme 1, the effective capacity of the battery is smaller than the normal capacity. When light is abundant, there is a waste of potential power due to abandoned light power, and when there is prolonged low light, there is a likelihood of power shortage due to a lower battery capacity. Scheme 1 cannot meet the reliability requirements of the power supply system (see Fig. 9(a)). In Scheme 2 for the PV (10 m^2) + Battery (72 kW · h) + RESOC (160 kW · h), thermal energy is generated as the RESOC works. Therefore, using a RESOC and battery combined energy supply, SOFC and SOEC can stabilize the ambient temperature and meet the optimal ambient temperature for battery operation. The combination of the two can meet the reliability of the system power supply as shown in Fig. 9(b). With Scheme 3, PV (10 m^2) + RESOC (160 kW · h), RESOC has a high operating temperature and is not affected by cold weather. When the photovoltaic power generation is weak, the SOFC supplies power to the oil and gas pipeline IoT monitoring platform. When the amount of photovoltaic power generation is greater than the load, the excess photovoltaic energy will be converted to hydrogen by SOEC for storage as shown in Fig. 9(c).

Combined with the analysis in Table VI, in the case of a low level of abandoned light power, the battery exhibits high economic efficiency due to high energy conversion efficiency, and has the ability to quickly balance power generation and load. Though both Scheme 2 and Scheme 3 can satisfy the reliability of the power supply, Scheme 2, which includes the battery, exhibits better economy. Therefore, Scheme 2 (PV + Battery + RESOC) is the preferred power supply scheme for

alpine-cold regions.

V. Conclusion

In this paper, the off-grid power supply system comprised of PV, battery, and RESOC is proposed for a remote and unattended oil and gas pipeline IoT monitoring platform. This paper establishes an optimization model for the operation of off-grid power supply systems and investigates the power model and SOFC of each component, the operating characteristic model of SOEC, and the operational reliability of the system. Three representative areas were selected (rainy areas, non-cold, low-rain areas, and alpine-cold areas) and three configurations (PV + Battery, PV + Battery + RESOC, PV + RESOC) were compared and analyzed. The MatlabCplex is used to solve the system operational optimization model. The results show that the configuration (PV + Battery + RESOC) is the preferred power supply scheme for rainy regions and alpine-cold regions. The (PV + Battery) configuration is the preferred power supply scheme for dry areas that are not cold and have high irradiance. In each area, the (PV + RESOC) configuration proves to be as reliable as the other configurations, but because RESOC's "electric-hydrogen-electric" integrated energy conversion efficiency is lower than that of a battery, its economy proved prohibitive. Overall, the work of this paper supports the optimization of the off-grid power system operation in different conditions. This will also provide guidance for future studies in system capacity configuration.

References

[1] National Bureau of Statistics, *Statistical Bulletin of National Economic and Social Development in 2018*. Beijing: National Bureau of Statistics, 2019.

[2] China Petroleum News Center. (2019, Feb. 28). 2018 domestic and international oil and gas industry development report [Online]. Available: http://www.stats.gov.cn/tjsj/zxfb/201902/t20190228_1651265.html

[3] Zhiyan Consulting Group. (2018, Dec. 26). 2019–2025 China Pipeline Inspection Engineering Industry Special Investigation and Development Prospect Forecast Report [Online]. Available: https://www.chyxx.com/research/201812/702601.html

[4] National Development and Reform Commission, National Energy Administration. (2017, May. 19). Medium and long-term oil and gas pipeline network planning [Online]. Available: http://www.ndrc.gov.cn/zcfb/zcfbghwb/201707/t20170712_854432.html

[5] Y. F. Zhu, L. Zhou, L. Geng, and H. F. Shi, "Application analysis of photovoltaic power system in oilfield," *Energy Conservation in Petroleum & Petrochemical Industry,* no. 4, pp. 49–51, Apr. 2014.

[6] Z. J. Cao, J. Lin, C. Wan, Y. H. Song, Y. Zhang, and X. H. Wang, "Optimal cloud computing resource allocation for demand side management in smart grid," *IEEE Transactions on Smart Grid,* vol. 8, no. 4, pp. 1943–1955, Jul. 2017.

[7] T. Ma, J. J. Cao, B. Zeng, and K. Liu, "Discussion on power supply scheme for modern gas pipeline station," *China Petroleum and Chemical Standard and Quality,* vol. 33, no. 5, pp. 248, 2013.

[8] H. T. Zhao, "Power supply scheme for RTU valve room of gas pipeline," *China Chemical Trade,* no. 12, pp. 45–46, Dec. 2012.

[9] B. S. Li, D. J. Tan, H. Li, Y. J. Cai, and N. Song, "Discussion on power supply scheme of remote pipeline RTU valve chamber," in *China International Oil and Gas Pipeline Conference*, 2011.

[10] P. Sun, "Use and maintenance of solar power supply system for long-distance oil and gas pipeline valve chamber," *China New Technologies and New Products*, no. 13, pp. 15, Jul. 2014.

[11] Z. Y. Chang, C. E. Si, H. H. Xu, S. X. Hu, Z. Z. Dai, and Y. Y. Yu, "Hybrid photovoltaic/wind generating system for pipeline cathodic protection," *Petroleum Planning & Engineering*, vol. 5, no. 1, pp. 47–48, Feb. 1994.

[12] Z. Y. Chang and S. X. Hu, "Wind/photovoltaic hybrid power generation system for cathodic protection of oil pipelines," *Energy of China*, no. 7, pp. 10–14, Jul. 1996.

[13] J. Lin, Y. Z. Sun, Y. H. Song, W. Z. Gao, and P. Sorensen, "Wind power fluctuation smoothing controller based on risk assessment of grid frequency deviation in an isolated system," *IEEE Transactions on Sustainable Energy*, Vol 4, no. 2, pp. 379–392, Apr. 2013.

[14] H. Jiang, J. Lin, Y. H. Song, W. Z. Gao, Y. Xu, B. Shu, X. M. Li, and J. X. Dong, "Demand side frequency control scheme in an isolated wind power system for industrial aluminum smelting production," *IEEE Transactions on Power Systems,* Vol. 29, no. 2, pp. 844–853, Mar. 2014.

[15] C. Wan, J. Lin, J. H. Wang, Y. H. Song, and Z. Y. Dong, "Direct quantile regression for nonparametric probabilistic forecasting of wind power generation," *IEEE Transactions on Power Systems,* vol. 32, no. 4, pp. 2767–2778, Jul. 2017.

[16] G. M. Xue, S. X. Hu, and J. H. Ma, "Application of photovoltaic power generation system in IOT of oilfield," *Instrumentation*, vol. 22, no. 1, pp. 94–96, Feb. 2015.

[17] Y. R. Yu, "Discussion on the advantages of applying wind-solar hybrid power generation system in the cut-off valve chamber of long-distance pipeline," *China Strategic Emerging Industry*, no. 20, pp. 61–62, May 2017.

[18] J. B. Greenblatt, "Opportunities for efficiency improvements in the U.S. natural gas transmission, storage and distribution system," Lawrence Berkeley National Laboratory, Berkeley, LBNL-6990E, 2015.

[19] J. Eze, C. Nwagboso, and P. Georgakis, "Framework for integrated oil pipeline monitoring and incident mitigation systems," *Robotics and Computer-Integrated Manufacturing*, vol. 47, pp. 44–52, Oct. 2017.

[20] T. C. Pharris and R. L. Kolpa, "Overview of the design, construction, and operation of interstate liquid petroleum pipelines," Argonne National Lab., Argonne, ANL/EVS/TM/08-1, 2007.

[21] Z. X. Liu, W. Qian, J. W. Guo, J. Zhang, C. Wang, and Z. Q. Mao, "Proton exchange membrane fuel cell materials," *Progress in Chemistry,* vol. 23, no. 2–3, pp. 487–500, Mar. 2011.

[22] W. W. Li, L. Li, and L. Yang, "Research progress of solid oxide fuel cell," *Chinese Journal of Power Sources,* vol. 40, no. 9, pp. 1888–1889, 1892, Sep. 2016.

[23] H. Bakhtiari and R. A. Naghizadeh, "Multi-criteria optimal sizing of hybrid renewable energy systems including wind, photovoltaic, battery, and hydrogen storage with ε-constraint method," *IET Renewable Power Generation,* vol. 12, no. 8, pp. 883–892, Nov. 2018.

[24] C. Wan, J. Lin, Y. H. Song, Z. Xu, and G. Y. Yang, "Probabilistic forecasting of photovoltaic generation: An efficient statistical approach," *IEEE Transactions on Power Systems,* vol. 32, no. 3, pp. 2471–2472, May 2017.

[25] L. M. Wei and X. Y. Lv, "Solid oxide fuel cell power generation system model and study on inverter simulation," *Power System Protection and Control*, vol. 44, no. 24, pp. 37–43, Dec. 2016.

[26] S. D. Ebbesen, S. H. Jensen, A. Hauch, and M. B. Mogensen, "High temperature electrolysis in alkaline cells, solid proton conducting cells, and solid oxide cells," *Chemical Reviews,* vol. 114, no. 21, pp. 10697–10734, Oct. 2014.

[27] S. J. Mou, J. Lin, X. T. Xing, and Y. Zhou, "Technology and application prospect of high-temperature solid oxide electrolysis cell," *Power System Technology*, vol. 41, no. 10, pp. 3385–3391, Oct. 2017.

[28] Q. Y. Jiang, Q. J. Shi, X. P. Li, Y. H. Chen, W. L. Zhang, and J. Y. Song, "Optimal configuration of standalone wind-solar-storage power supply system," *Electric Power Automation Equipment*, vol. 33, no. 7, pp. 19–26, Jul. 2013.

[29] C. H. Huang, "The use of solar energy in oil and gas pipelines," *Oil-Gasfield Surface Engineering*, vol. 31, no. 11, pp. 8–10, Nov. 2012.

[30] L. Zhang, X. B. Wei, and G. Zhang, "Analysis of the relationship between temperature and capacity on sealed valve-regulated lead-acid battery," *Diesel Locomotives*, no. 9, pp. 19–20, 26, Sep. 2007.

[31] "Selection and basic calculation of solar power system in natural gas long distance pipeline engineering," pp. 6–9, May. 2015.

[32] H. Jiang, J. Lin, Y. H. Song, and D. J. Hill, "MPC-based frequency control with demand-side participation: A case study in an isolated wind-aluminum power system," *IEEE Transactions on Power Systems,* vol. 30, no. 6, pp. 3327–3337, Nov. 2015.

[33] J. H. Ge and L. Wan, "Power supply scheme analysis for remote control block valve station of long distance pipeline," *Electric Engineering*, no. 11, pp. 125–127, Jun. 2018.

[34] C. G. Wang and S. C. Wang, "Cathodic protection of oil and gas transmission pipeline - design and construction of solar power system in tarim oilfield," *Solar Energy,* no. 2, pp. 11–13, Jun. 1997.

[35] S. J. Gao, "A low-power solution of security and defense system of oil & gas pipeline valve chamber," *Energy Conservation in Petroleum & Petrochemical Industry*, vol. 8, no. 11, pp. 32–35, Nov. 2018.

Chenxing Xu received the MAE degree in Information Engineering from Zhejiang A&F University, China, in 2020. Her main research interests include Off-grid multi-energy complementary system and Oil and gas pipeline monitoring system power supply system.

Jian Wu received Ph.D. degree in the Department of Chemical and Biochemical Engineering from Technical University of Denmark, Denmark, in 2012. He is currently an associate professor in the College of Information Engineering of Zhejiang A&F University, Hangzhou, China. His main research interests include low carbon technology, energy conversion devices and smart energy system.

Hailin Feng received Ph.D. degree in the department of Computer Application Technology from University of Science and Technology of China, China, in 2007. He is currently a professor and associate dean of the College of Information Engineering, Zhejiang A&F University, Hangzhou, China. His research interests include intelligent signal and information processing, energy internet, non-destructive testing, and embedded system design.

Andreas Ibrom received Ph.D. degree in University of Gottingen, and is currently a professor in the Department of Environmental Engineering of Technical University of Denmark, Denmark. His research interests include turbulence measurement and data post-processing, biophysical and dynamic ecosystem modeling, data analysis, and scientific programming.

Qing Zeng received Ph.D. degree in the Department of Energy Technology from Aalborg University, Denmark, in 2018. He is currently a Research Fellow in Sichuan Energy Internet Research Institution of Tsinghua University, Chengdu, China. His research interests include smart energy system, hydrogen fuel cell and Electric energy storage.

Jianfeng Zhang received Ph.D. degree in the department of Biosystem Engineering from Zhejiang University, China, in 2014. He is currently a lecturer at the College of Information Engineering, Zhejiang A&F University, Hangzhou, China. His research interests include agricultural IoT, rural power and new energy generation.

Na Li received the M.Sc. degree at Wind Energy department of Technical University of Denmark in 2009. She was Research Assistant at Risø DTU between 2007 and 2010, and worked as Engineer at MingYang Wind Power European R&D Center and MHI Vestas Offshore Wind from 2010 to 2017. She is currently the Chief Representative of CRRC Wind Power (Shandong) Co., Ltd Representative Office in Denmark. Her research interests include ower supply, wind & site, wind loads, blade test.

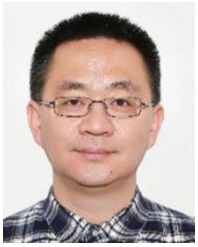

Qiang Hu received his Ph.D. degree in the Department of Energy Conversion of Technical University of Denmark (DTU). He is currently a co-founder and CTO of Zhejiang Zhentai Energy Tech. Co. Ltd.. His research interests include electrochemistry, material, chemical engineering and process design.